

## Self-organization of jets in electrospinning from free liquid surface: A generalized approach

David Lukas,<sup>a)</sup> Arindam Sarkar,<sup>b)</sup> and Pavel Pokorný<sup>c)</sup>

*Technical University of Liberec, Faculty of Textiles, Department of Nonwoven Textiles, Halkova 6, Liberec 1, 461 17, Czech Republic*

(Received 12 November 2007; accepted 16 February 2008; published online 25 April 2008)

Electrospinning has enabled creation of excellent materials for a great number of applications. Previously, it was based on less productive capillary spinners. The present study is based on recent efforts to elevate electrospinning technology to an industrial level by simultaneously provoking innumerable polymeric jets from a sufficiently large liquid surface to increase productivity. Particularly, it deals with electrospinning from free surface of conductive liquids and validates a formulated hypothesis that explains self-organization of jets on one-dimensional free liquid surfaces in terms of electrohydrodynamic instability of surface waves. Here, it is shown how the hypothesis, based on a profound analysis of a dispersion law, explains that above a certain critical value of applied electric field intensity/field strength the system starts to be self-organized in mesoscopic scale due to the mechanism of the “fastest forming instability.” The mechanism plays a key role in selecting a particular wave with a characteristic wavelength whose amplitude boundlessly grows faster than the others. The fastest growing stationary wave, according to the hypothesis, marks the onset of electrospinning from a free liquid surface with its jets originating from the wave crests. Singularity of this approach lies in predicting critical values of the phenomenon, viz., critical field strength and corresponding critical interjet distance. The critical field strength, will, thereafter, be used in defining a unique dimensionless electrospinning number. It will, subsequently, be shown how the critical interjet distance, i.e., the maximal distance between the neighboring jets, simply depends on the capillary length. The capillary length represents a latent characteristic spatial scale of the system. The theory also predicts interjet distance for field strengths above the critical value. The said prediction is universally applicable for all conductive liquids if it is expressed in terms of the dimensionless parameters of the interjet distance and the electrospinning number. The theory also predicts relaxation time, necessary for spontaneous jetting after a high voltage is applied. The theoretical considerations are eventually compared to that of Zeleny’s, obtained for capillary electrospinner to demonstrate universality of the approach. Eventually, jetting from free liquid surface on specially designed linear cleft electrospinner are observed, analyzed, and compared to the theoretical predictions obtaining satisfactory results. © 2008 American Institute of Physics. [DOI: 10.1063/1.2907967]

### INTRODUCTION

Electrospinning, one of the most popular nanotechnologies, has enabled creation of excellent materials for application in tissue engineering,<sup>1,2</sup> drug delivery,<sup>3,4</sup> wound dressings, filters,<sup>5,6</sup> heat, and sound insulators. Previously, it was based on less productive needle or capillary spinners.<sup>7–9</sup> Subsequently, effort was focused in enhancing the productivity by provoking numerous polymeric jets through needleless methods, i.e., methods where polymeric jets are spontaneously created from liquid surfaces.<sup>10,11</sup>

Electrospinning, based on self-organization of nanoscale fibers from polymeric liquids in high voltage fields, resembles, in some ways, biological processes wherein natural nanofibers such as cellulose and collagen organize

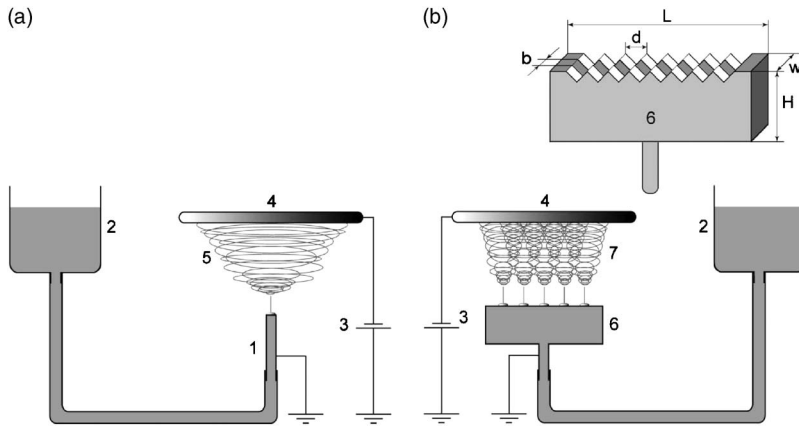
themselves.<sup>12</sup> Unlike classic spinning technologies, electrospunners are free of complex moving as well as passive mechanical components. Various phenomena, such as jetting, jet whipping, and drying, originating from electrohydrodynamics, have substituted conventional methodologies that are used in designing common fiber-spinning machines. Self-organization and drawing of polymeric jets to nanoscale via electrospinning have, thus, successfully revolutionized spinning technology.

Electrospinning and closely related phenomena of liquids were observed at the beginning of the former century<sup>8,13</sup> with apparatuses, as depicted and described in Fig. 1(a). Polymer jets were formed on tips of needles, due to imbalance between capillary and electric forces, i.e., when the applied voltage  $V$  exceeded a critical value, jetting of polymer solution was initiated. The critical voltage  $V_c$  (in kilovolts) for a liquid, having a surface tension  $\gamma$  in a capillary of radius  $r$ , kept at a distance  $h$  from the collector with zero hydrostatic pressure was estimated by Taylor and Van Dyke<sup>7</sup> as

<sup>a)</sup> Author to whom correspondence should be addressed. Electronic mail: david.lukas@tul.cz. Fax: +420-48-535-3244. Tel.: +420-48-535-146 and +420-606-639-586.

<sup>b)</sup> Electronic mail: sarkararindam@iitdalumni.com.

<sup>c)</sup> Electronic mail: pavel.pokorny@tul.cz.



$$\sqrt{4 \ln\left(\frac{2h}{r}\right) \pi r \gamma 1.30(0.09)} < V_c < \sqrt{4 \ln\left(\frac{4h}{r}\right) \pi r \gamma 1.30(0.09)}. \quad (1)$$

In order to widely commercialize electrospinning, effort has been given either in using multiple capillaries,<sup>14</sup> where each of the capillaries produces a jet or to provoke numerous jets from a liquid surface. Incidentally, the notion for the later was primarily brought about by Yarín and Zussman<sup>11</sup> under the phrase of “needleless electrospinning.” Generally, various electric field concentrators accompany needleless electrospinning. Yarín and Zussman applied strong magnetic field on a magnetic liquid to induce many spikes. The spikes became field concentrators and led to a huge increase of jet numbers, and consequently, to the growth of fiber production. Subsequently, another idea, based on an observation that jets rise up even from free and nearly flat liquid surfaces<sup>10</sup> led to massive production of nanofibres and consequent commercialization of the technology under the brand name of Nanospider™.<sup>15</sup> This technology is not only the first one to be successful at industrial scale but from the standpoint of its simplicity and its ability to utilize the perfect balance and symmetry of nature, it seems to have immense potential in the contemporaneous development of innumerable associated nanotechnologies as well as comprehensive understanding of some of the yet unknown mysteries of nature. A slowly rotating horizontal cylinder, covered with thin layer of a polymeric solution, serves here as a field concentrator. Particularly, the relevant physical principle of electrospinning will be investigated here both theoretically and experimentally using a cleft made from metallic plates, as sketched and described in Fig. 1(b). The cleft itself serves here as a field concentrator and resembles the simplest model of the process, where jets self-organize on a very narrow, nearly one-dimensional, free liquid surface, confined between the plates.

Although needleless electrospinning from free liquid surfaces has evolved as an enormously promising technology and has even been very recently industrially implemented, the theoretical description of this phenomenon has not been formulated yet, as opposed to the relatively well-described conventional capillary electrospinning, viz., Taylor’s Eq. (1).

FIG. 1. Capillary and cleft electrospinning: (a) capillary electrospinning consists of a needle/capillary (1) that is connected to a container (2), filled with polymer solution, through a flexible tube. A high voltage source (3) generates electrostatic field in the region between the needle and a collector (4). Whipping jet (5) transports the polymer solution from the needle to the disk collector on which nanofibers are collected in layers. The difference in the liquid levels of the container and the needle rim provides a hydrostatic pressure. (b) In a cleft electrospinning, the needle is replaced by two metallic plates (6) of length  $L$ , height  $H$ , and a cleft of breadth  $b$  between them. The outer width of the cleft is  $w$ . Upper edges of both the plates are serrated as shown in the magnified upright part (6). Several polymeric jets (7) are created on a free liquid surface when sufficient field strength is applied.

The present endeavour initially strives to frame a hypothesis concerning electrohydrodynamic evolution of jets in collection from a free liquid surface under an external electrostatic field, and then the governing law of their dispersion is carefully analyzed from the standpoint of the hypothesis. The main theoretical results (critical field strength, critical distance between neighboring jets, the dependency of the inter-jet distance and the dependency of the relaxation time on the field strength) are formulated thereafter. The experimental part compares theoretical outputs with measured data. It will also be shown that the theory amazingly predicts even the critical field strengths obtained for capillary electrospinning. However, the main thrust will be directed toward the analysis of experimental data, obtained through cleft electrospinning and their comparison with theoretical predictions. Finally, conclusive remarks summarize the work and further applications of the current theoretical approach in the parlance of electrospinning have been suggested.

## THE HYPOTHESIS

Electrohydrodynamics of a liquid surface may conveniently be analyzed with the waves running on an one-dimensional approximation of the fluid surface, confined in an extremely narrow and infinitely deep cleft between two infinitely long plates that are oriented along the horizontal axis (say,  $x$  axis) of a three-dimensional rectangular Cartesian system. This one-dimensional model is, perhaps, topologically the simplest one for further theoretical as well as experimental investigation of the present problem. The wave’s vertical displacement along the  $z$  axis is described using the periodic real part of a complex quantity  $\xi$ ,

$$\xi = A \exp[i(kx - \omega t)]. \quad (2)$$

The symbols  $A$ ,  $k$ ,  $\omega$ , and  $t$  stand for the amplitude, wave number, angular frequency, and the time, respectively. The liquid in the cleft is subjected to fields of gravitation and electricity in addition to capillary effects, caused by nonzero curvature of its surface. The related dispersion law, as will be subsequently shown in Eq. (7), reveals that square of the angular frequency  $\omega^2$  depends on the gravitational acceleration  $g$ , wave number  $k$ , field strength  $E_0$ , liquid surface tension  $\gamma$ , and the liquid density  $\rho$ . For a particular liquid, the critical parameter to initiate jetting is the field strength  $E_0$ . When  $E_0$  exceeds a critical value  $E_c$ , the square of the angu-

lar frequency  $\omega^2$  becomes negative and so,  $\omega$  becomes purely imaginary. The imaginary angular frequency, defined as  $q = \text{Im}(\omega)$ , then abruptly changes the behavior of the superficial waves that obey the following relation:

$$\xi = Ae^{qt} \exp(ikx). \quad (3)$$

The entity  $q = \text{Im}(\omega)$ , then quantitatively delimits apprehension of the angular frequency. It starts to be responsible for exponential growth of the amplitude since it “migrates” from the argument of harmonic function to the amplitude part of the displacement  $\xi$ , where it causes the exponential wave growth. Moreover, the growing waves simultaneously start to become spatially stationary since the wave described by Eq. (3) has lost its time dependence in the argument of its exponential part. Waves with different wave numbers  $k$  at the stable condition subside as the critical value of the field strength is attained since the one with maximum growth factor  $q$  prevails. It is worth mentioning that the quantity reciprocal to the growing factor  $q$  is a relaxation time  $\tau$ , i.e.,  $\tau = 1/q$ . The relaxation time is the time that characterizes the appearance of the electrospun jets after the electrostatic field is switched on. More precisely, after the relaxation time  $\tau$ , the amplitude  $A$ , increases  $e$  times, where  $e \cong 2.718$  is the basis of natural logarithm. Hence, it follows the hypothesis that exponential growth of the amplitude characterizes electrohydrodynamic formation of electrospinning jets on free liquid surfaces. This phenomenon may also be recognized as self-organization on the basis of the “fastest forming instability.”<sup>16</sup>

## DISPERSION LAW

The Euler equation, followed by the works of Landau and Lifshitz,<sup>17,18</sup> appropriately brings about the dispersion law, as will be derived soon. The Euler equation is as follows:

$$\rho \frac{d\vec{v}}{dt} + \nabla p = 0. \quad (4)$$

In the above context, it is noteworthy that the liquid’s movement satisfies a velocity field,  $\vec{v} = \vec{v}[x(t), y(t), z(t), t]$ , and  $p$  denotes the liquid pressure. Since the analysis of the phenomenon demands some simplification, it is assumed, henceforth, that the conductive liquid is an incompressible one, i.e.,  $\rho$  is constant, and the amplitude  $A$  of the wave is initially negligibly small, as compared to its wavelength  $\lambda$ . Since jets evolve from wave crests; the amplitudes are, at their later stages of time evolution, at least comparable to their wavelength. This seemingly ostensible contradiction with the above-formulated assumption will be eventually detailed in this paper. If  $a \ll \lambda$ , the liquid flow is a potential one, i.e.,  $\nabla \times \vec{v} = 0$  and the time derivative of the velocity  $d\vec{v}/dt$  can be approximated with its partial derivative  $\partial\vec{v}/\partial t$ . Since  $\nabla \times \vec{v} = 0$ , it follows that a scalar velocity potential  $\Phi$  can be introduced, such that  $\vec{v} = \nabla\Phi$ . These aspects simplify the Euler equation into the following form:

$$\nabla \left( \rho \frac{\partial\Phi}{\partial t} + p \right) = 0. \quad (5)$$

Equation (5) is further reshaped to be appropriate especially for the investigation of the liquid surface dynamics. The pressure  $p$  on the liquid surface consists of the components of hydrostatic pressure  $p_h = \rho g \xi$ , capillary pressure  $p_c = -\gamma(\partial^2 \xi / \partial x^2)$ , and electric pressure  $p_e$ . The last one appears due to interaction between induced charges on the liquid surface and the external electric field. The pressure  $p_e$  is proportional to the square of the field strength on the liquid surface, i.e.,  $p_e = \frac{1}{2} \epsilon E^2$ , where  $\epsilon$  is the electric permittivity of the ambient gas. The total field strength  $E$  may be derived from two components of the total electric potential  $\varphi$ . The first component  $\varphi_0$  is the potential of an ideally flat, calm liquid surface. The other one  $\varphi_1$  is due to perturbation, caused by tiny surface waves. These potentials resemble zero and first Fourier components of the total field of a grid of parallel and equidistant wires,<sup>19</sup> i.e.,  $\varphi_0 = -E_0 z$  and  $\varphi_1 = \text{const} \exp(-kz) \exp[i(kx - \omega t)]$ . Near the liquid surface, the total potential  $\varphi$  is constant, and for convenience, it was chosen to be zero, i.e.,  $\varphi_1(\xi) = -\varphi_0(\xi) = E_0 \xi$ . Corresponding field strengths  $E_0$  and  $E_1$  are easily calculated from the potentials  $\varphi_0$  and  $\varphi_1$ , using the formula  $E = -\nabla\varphi$ . Assuming that  $E_0 \gg E_1$ ,  $p_e$  can be expressed as  $p_e = \frac{1}{2} \epsilon E^2 \cong \frac{1}{2} \epsilon E_0^2 + \epsilon E_0^2 k \xi$ .

Thus, taking into account all the previously mentioned pressure components  $p_h$ ,  $p_c$ , and  $p_e$ , whose gradients are non-zero, the boundary condition at the liquid surface reshapes as

$$\rho \frac{\partial\Phi}{\partial t} \Big|_{z=\xi} + \rho g \xi - \gamma \frac{\partial^2 \xi}{\partial x^2} - \epsilon E_0^2 k \xi = 0. \quad (6)$$

The velocity potential  $\Phi$  on the liquid surface, i.e., for  $z = \xi \cong 0$ , and the vertical velocity component  $v_z$  of the liquid surface are related as  $v_z = \partial\xi/\partial t = \partial\Phi/\partial z|_{z=0}$ . Also, the term  $\partial\xi(x, t)/\partial t$  may be expressed as  $-i\omega A \exp[i(kx - \omega t)]$ . Since,  $\Phi$  quenches with  $z \rightarrow -\infty$ ,  $\Phi(x, z, t)$  is supposed to be of the form  $\Phi(x, z, t) = B \exp(+kz) \exp[i(kx - \omega t)]$ , thus, implying,  $\partial\Phi(x, z, t)/\partial z|_{z=0} = kB \exp[i(kx - \omega t)]$ . It has to be highlighted that the limit  $z \rightarrow -\infty$  for quenching  $\Phi$  entails the assumption of infinite depth of the liquid. From the condition  $\partial\xi(x, t)/\partial t = \partial\Phi(x, z, t)/\partial z|_{z=0}$  it follows immediately that  $B = -i\omega A/k$ . Using Eq. (6) along with derived expressions for  $\Phi$  and that for  $B$ , a dispersion law for  $\omega^2$  is presented as

$$\omega^2 = (\rho g + \gamma k^2 - \epsilon E_0^2 k) \frac{k}{\rho}. \quad (7)$$

## ANALYSIS OF THE DISPERSION LAW

Positivity of  $\omega^2$  for each value of the wave number  $k$  necessarily ensures stability. So, the liquid surface for subcritical field strength has “running” waves of constant amplitude with different values of  $k$  and their corresponding  $\omega$ ’s. However, for field strengths higher than the critical one, the calculation of  $k$ ’s, for which  $\omega^2$  is negative and minimal, is crucial. The criticality sets in at  $\omega^2 = 0$  with simultaneous condition  $\partial\omega/\partial k = 0$ . Referring Eq. (7), i.e., the dispersion law, for  $\omega^2(k) = 0$ , the wave number of a growing wave  $k$  reaches its minimal/critical value when  $k_c = \epsilon E_0^2 / 2\gamma$ . Substi-

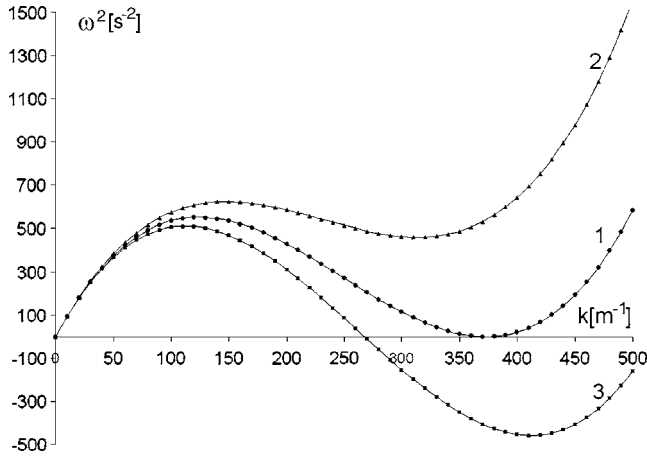


FIG. 2. Relationship between the square of the angular frequency and the wave number for distilled water: curves 1, 2, and 3 represent relationships between the square of the angular frequency  $\omega^2$  and the wave number  $k$ , for field strength values,  $E=E_c=2.461\,945\,094 \times 10^6$  V/m,  $E=2.4 \times 10^6$  V/m, and  $E=2.5 \times 10^6$  V/m, respectively. Critical wave number is  $k_c=3.726\,77 \times 10^2$   $\text{m}^{-1}$  as is evident from curve No. 1. The values of water surface tension  $\gamma$ , water density  $\rho$ , gravity acceleration  $g$ , and electric permittivity  $\epsilon$  used for the plot are  $\gamma=72 \times 10^{-3}$  N/m,  $\rho=10^3$  kg/m<sup>3</sup>,  $g=10$  m/s<sup>2</sup>,  $\epsilon=8.854 \times 10^{-12}$  m<sup>-3</sup> kg<sup>-1</sup> s<sup>4</sup> A<sup>2</sup>.

tuting  $k_c$  for  $k$  in Eq. (7) gives the range of the field strength  $E_0$  for stable waves as  $E_0^4 < 4\gamma\rho g/\epsilon^2$ . Hence, the critical field strength  $E_c$  for unstable waves is given as

$$E_c = \sqrt[4]{4\gamma\rho g/\epsilon^2}. \quad (8)$$

From Eq. (8) follows a threshold condition of  $\frac{1}{2}\epsilon E_c^2 = \frac{\gamma}{a}$ , where  $a = \sqrt{\gamma/\rho g}$  is the capillary length, frequently used in colloid chemistry<sup>20</sup> and wetting theory.<sup>21</sup> Accordingly, the threshold condition may be interpreted as the equilibrium of the pressures due to electric forces  $\frac{1}{2}\epsilon E_c^2$  and that of the capillary forces  $\frac{\gamma}{a}$ , following the Young–Laplace equation, where the role of a mean surface curvature is played by  $1/a$ . The capillary length represents the hidden/latent characteristic length scale of needleless electrospinning from free liquid surfaces. Moreover, it is convenient, as will be shown further in formulation of the Eq. (10), to define a dimensionless electrospinning number  $\Gamma$  as  $a\epsilon E_0^2/2\gamma$ , which differs from the one introduced by Shenoy *et al.*<sup>22</sup> Using this definition, electrospinning is initiated only if  $\Gamma \geq 1$ , its critical value reaches  $\Gamma_c = 1$ . The critical field strength  $E_c$  for distilled water, having permittivity of  $\epsilon = \epsilon_0 = 8.854 \times 10^{-12}$  m<sup>-3</sup> kg<sup>-1</sup> s<sup>4</sup> A<sup>2</sup> is calculated as  $E_c = 2.46195 \times 10^6$  V/m. Minimal and negative square values of the angular frequency  $\omega^2$  correspond to the maximal growth factors  $q$ 's inherently connected with the self-organization caused by the mechanism of the fastest forming instability. The minimal value of  $\omega^2$  with respect to  $k$  is obtained by solving  $d\omega^2/dk=0$ , thus, obtaining two solutions  $k_1$  and  $k_2$ , that are expressed together as

$$k_{1,2} = \frac{2\epsilon E_0^2 \pm \sqrt{(2\epsilon E_0^2)^2 - 12\gamma\rho g}}{6\gamma}. \quad (9)$$

Referring to Fig. 2, minimum of  $\omega^2$  occurs at that value of  $k$ , whichever is greater. Since the average interjet distance is described in terms of the wavelength  $\lambda = 2\pi/k$ , its depen-

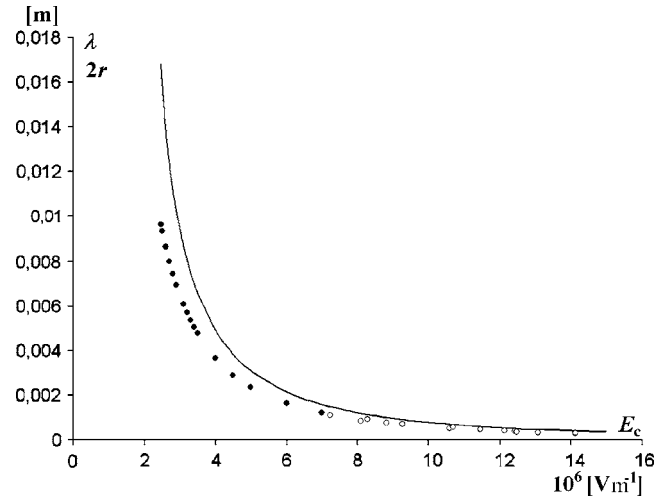


FIG. 3. Dependence of the wavelength  $\lambda$  on the critical field strength,  $E_c$ . The  $\lambda$ – $E_c$  relationship, according to Eq. (9) is plotted for distilled water with permittivity  $\epsilon=8.854 \times 10^{-12}$  m<sup>-3</sup> kg<sup>-1</sup> s<sup>4</sup> A<sup>2</sup>. Critical field strengths, according to Zeleny's observations (Ref. 8) are plotted for capillary radii  $r$  up to  $r=0.543$  mm with empty circles. They have a standard deviation of about 2%. For greater capillary radii, Zeleny's extrapolation, according to the formula  $E\sqrt{r}=56.9 \times 30\,000$  V m<sup>-1/2</sup>, is used to plot the point with bold circles. The comparison is based on the relationship  $\lambda \approx 2r$ . All experimental data are plotted for distilled water with surface tension  $\gamma$  of 72 mN/m, negligibly small hydrostatic pressure and ambient temperature close to 22 °C.

dency on  $E_0$ , as sketched in Fig. 3, is governed by the relation  $\lambda = 12\pi\gamma/[2\epsilon E_0^2 + \sqrt{(2\epsilon E_0^2)^2 - 12\gamma\rho g}]$ . This can be more comprehensively expressed using the capillary length  $a$  and the previously introduced electrospinning number  $\Gamma$  as  $\lambda = 3\pi a/(\Gamma + \sqrt{\Gamma^2 - 3/4})$ . Therefore, the critical wavelength of  $\lambda_c = 2\pi/k_c = 2\pi a$  may directly and easily be expressed with the capillary length  $a$ . For distilled water holds  $\lambda_c = 1.685\,96 \times 10^{-2}$  m. The relation between dimensionless intra-jet distance  $\Lambda = \lambda/a$  and  $\Gamma$  given below

$$\Lambda = \frac{3\pi}{\Gamma + \sqrt{\Gamma^2 - 3/4}} \quad (10)$$

is universal for needleless electrospinning of all conductive liquids and is used here to draw the graph in Fig. 4. The critical value of the dimensionless intra-jet distance is  $\Lambda_c = 2\pi$ .

To derive the relationship between the relaxation time  $\tau$  and the electrospinning number  $\Gamma$ , it is convenient to start with the dimensionless wave number  $K = 2\pi/\Lambda = ak$  that belongs to the fastest growing wave. Both the dimensionless wave number  $K$  and the dimensionless wavelength  $\Lambda$  are only functions of the electrospinning number, as evident from Eq. (10). The dispersion law (7), when expressed with  $K$  and  $\Gamma$ , takes the form of  $\omega^2 = \frac{g}{a}K(1 - 2K\Gamma + K^2)$ . The term  $1 - 2K\Gamma + K^2$  from the right hand side of the relation can be rewritten as  $\frac{2}{3}(1 - K\Gamma)$  using the definition of  $K$ . Thus,  $\tau$  may be represented as  $\tau = 1/\text{Im}(\omega) = \sqrt{a/g}\sqrt{3/2K(K\Gamma - 1)}$ . The quantity  $\sqrt{a/g}$  represents a characteristic time scale of the system and, hence, a relation between dimensionless relaxation time  $T = \tau/\sqrt{a/g}$  and electrospinning number  $\Gamma$  can be expressed as comprehensively as

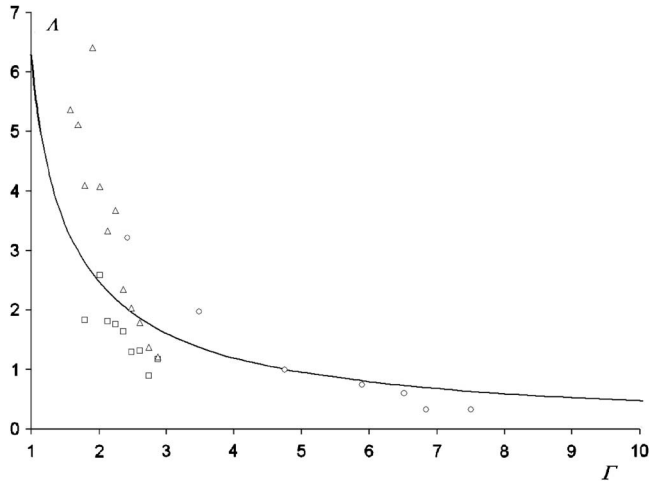


FIG. 4. Universal curve showing dependency of the dimensionless wavelength  $\Lambda$  on the electrospinning number  $\Gamma$ : three series of experimental data, distinguished here using various symbols, were obtained using measurements carried out with linear clefts using polyvinyl-alcohol solutions. Circles belong to the distance between the upper edge of the cleft and collector  $70 \pm 3$  mm, the distance  $80 \pm 3$  mm is assigned to squares and, ultimately, triangles represent the distance  $90 \pm 3$  mm. Standard deviations of  $\Lambda$  are in the interval from 0.8 up to 2. The solid, continuous line is plotted according to Eq. (9) for  $\gamma=0.48$  mN/m,  $\epsilon=8.854 \times 10^{-12}$  m<sup>-3</sup> kg<sup>-1</sup> s<sup>4</sup> A<sup>2</sup> and solution density  $\rho=879.5$  kg m<sup>-3</sup>  $\pm$  0.5 kg m<sup>-3</sup>, i.e.,  $a=0.00234$  m.

$$T = \sqrt{\frac{3}{2K(K\Gamma - 1)}}. \quad (11)$$

The dependence of  $T$  on  $\Gamma$  is plotted in Fig. 5. This relationship is universal for all conductive liquids and holds for  $\Gamma \geq 1$ . The characteristic time scale  $\sqrt{a/g}$  is of the order of time during which a body travels through a distance, equivalent to the capillary length  $a$  after it is released and to have a free fall under gravity.

## EXPERIMENTAL

Apparently, now it seems that there exist two parallel theories explaining an onset of electrospinning: Taylor's for capillary spinners and the one framed here for electrospinning from free liquid surfaces. On the contrary, electrospinning as a phenomenon exists in its unity, independently on

any theoretical tool used for its investigation and description. Presently keeping this aspect in mind, the critical field strength for electrospinning from free liquid surface  $E_c$  is first compared to  $E_c$ 's for distilled water jets from capillaries of various radii  $r$ , measured by Zeleny,<sup>8</sup> shown in Fig. 3. In his experiments, Zeleny applied no hydrostatic pressure to the liquid in the capillary, thus, meeting a system of assumptions in the present case. It is assumed for this moment that electrospinning from a needle/capillary in conventional electrospinning may occur only under the condition that the needle diameter  $2r$  is equal to the wavelength of the fastest growing wave, predicted by the newly introduced theory of free liquid surface electrospinning. Critical field strengths, according to Zeleny's observations, are plotted for capillary radii  $r$  up to  $2r=1.086$  mm. For greater capillary radii, Zeleny's extrapolation is used according to the formula  $E\sqrt{r} = 56.9 \times 30\,000$  V m<sup>-1/2</sup>.<sup>8</sup> Critical field strength values predicted by the present theory and Zeleny's experimental data set are quite comparable. Therefore, the theory in question and the above assumption that the critical field strength value  $E_c$  allows the creation of surface wave whose wavelength  $\lambda$ , predicted using the above mentioned formula  $\lambda = 12\pi\gamma/[2\epsilon E_c^2 + \sqrt{(2\epsilon E_c^2)^2 - 12\gamma\rho g}]$ , is equal to the capillary diameter  $2r$ , are positively confirmed.

In Fig. 4, dimensionless wavelength  $\Lambda$  versus electrospinning number  $\Gamma$  is plotted with experimental data, obtained from linear clefts where aqueous solutions of polyvinyl alcohol were spun. Polyvinyl alcohol, Sloviol-R were purchased from Novacke chemicke zavody, Novaky, Slovakia, with predominant molecular weight 60 000 g/mol, having the viscosity of 10.4 mPa s for 4% aqueous solution. Fresh 8% solutions were prepared by dissolving the Polyvinyl alcohol in distilled water. For the stabilizing the solutions' surface tension, 2% (v/v) butyl alcohol was added. Surface tension  $\gamma$  of the solution was 48 mN/m. The temperature during the observations was  $21 \pm 2$  °C and the relative moisture was  $(73 \pm 2)\%$ . The solution density  $\rho$  was  $879.5 \pm 0.5$  kg m<sup>-3</sup>.

Electrospinning of free liquid surface was carried out with stainless steel linear cleft, having outer length  $L = 70.46 \pm 0.07$  mm, inner length of  $60.03 \pm 0.03$ , height  $H = 20.08 \pm 0.02$  mm, breadth  $b=0.30 \pm 0.2$  mm, and outer

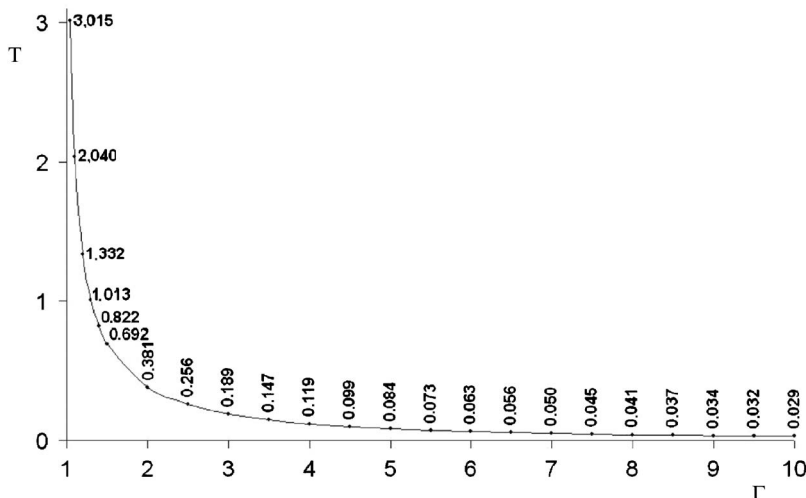


FIG. 5. Universal curve showing dependency of dimensionless relaxation time  $T$  on the electrospinning number  $\Gamma$ .

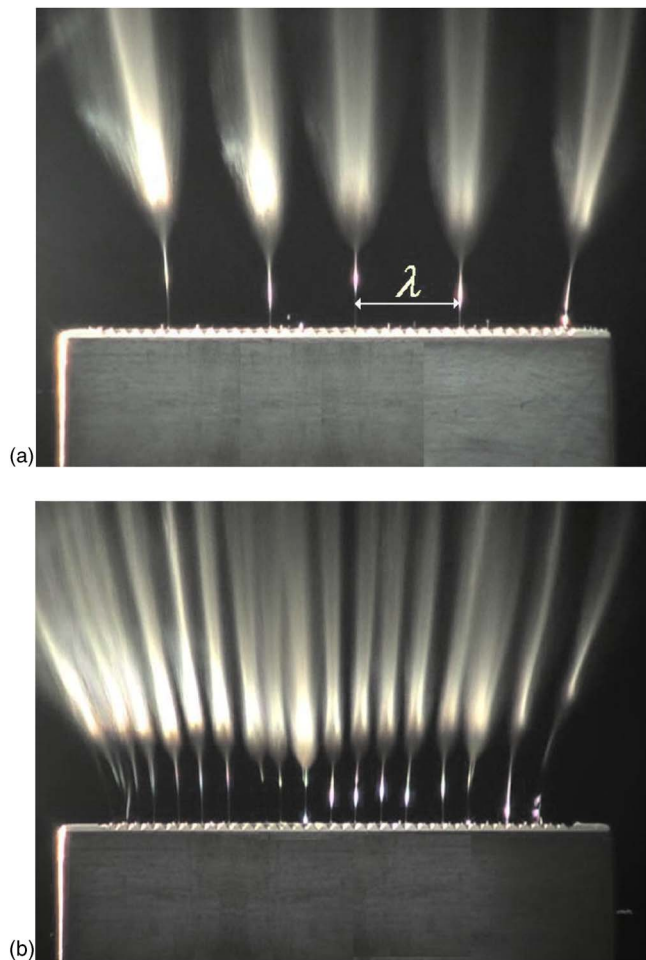


FIG. 6. (Color online) Linear clefts emit polymeric jets. Clefts in (a) and (b) emit polymeric (polyvinyl alcohol) jets at the voltages, 32 and 43 kV, respectively. The interjet distance/wavelength is  $\lambda$ . The distance between the cleft and the collector was adjusted at  $80 \pm 2$  mm.

width  $w = 2.87 \pm 0.02$  mm. Upper edges of both the plates were serrated. The serrations hinder spilling of the polymeric solution from the cleft to a certain extent. Distance  $d$  between neighboring teeth was  $1.68 \pm 0.02$  mm and their height was  $2.03 \pm 0.003$  mm. These sawlike patterns do not serve as main field concentration points since liquid surfaces before electrospinning onsets were as a rule above them. One has to admit, on the other hand, there is a weak but not strict correlation between sawlike structure of the cleft and jet positions that can gently influence measurements. The process run quite similarly with completely smooth cleft upper edges but liquid spilling was not under control. The clefts were designed and precisely manufactured by Vanicek, Smrzovka, Czech Republic. The clefts, emitting polymeric (polyvinyl alcohol) jets at the voltages of 32 and 43 kV, are portrayed in Fig. 6. The circular metallic collector had diameter of  $149.9 \pm 0.1$  mm. The distance between the cleft and the collector was kept at distances of 70–90 mm. The distance was constant for each series of experiments. Specifications of the high voltage source used were 300 W high voltage dc power supply with regulators; model number PS/ER50N06.0-22; manufactured by Glassman High Voltage, Inc.; output parameters of 0–50 kV, 6 mA. The collector of the setup was connected to the negative pole of the high voltage source

while the cleft was grounded. Linear clefts were supplied with polymeric solution at volume rate of 6–15 ml/h using linear pump or with hydrostatic pressures corresponding to 15–55 cm of water column. Field strengths in Fig. 4 were calculated from voltage values assuming a linear relationship between them for particular spinner geometry representing particular distance between the cleft and the collector. The proportionality constant was determined from the critical voltage, i.e., the lowest voltage for which jets appear, and from the critical field strength value predicted by Eq. (8). The dependence of the dimensionless wavelength on the electrospinning number, viz., Fig. 4, from the theoretical prediction is qualitatively similar to that obtained from experiments. Standard deviations of experimental data, i.e., of  $\Lambda$ , are, however, large as compared to corresponding average values since the system is enormously sensitive to a large number of parameters, such as surface tension and concentration fluctuations, mutual adjustment of the position of the cleft and collector, feeding rate of the cleft with the polymeric solution, and curvature of the liquid surface in the cleft.

## CONCLUSION

The present one-dimensional electrohydrodynamic theory of electrospinning from free surfaces of conductive liquids seems to complement the existing analysis of capillary electrospinning<sup>23</sup> introduced by Taylor. While Taylor<sup>7</sup> mainly concerned geometry of a liquid cone and critical voltage in the context of electric and capillary pressures acting there at equilibrium, this one adds a more generalized approach toward studying dynamics of surface waves. This approach leads to the discovery of the pair of electrospinning fundamental parameters, such as capillary length  $a$  and characteristic time scale  $\sqrt{a/g}$ . Also, a set of three inherent dimensionless quantities is defined. These are electrospinning number  $\Gamma$ , dimensionless wavelength  $\Lambda$ , and dimensionless relaxation time  $T$ , which efficiently characterize the process. Using those five tools (parameters and dimensionless quantities), the theoretical description of electrospinning is extremely comprehensive. The criticality appears for universal value of the electrospinning number  $\Gamma_c = 1$ . The dimensionless wavelength in criticality is also universal for all conductive liquids  $\Lambda_c = 2\pi$ . The theory is able to describe the dimensionless interjet distance  $\Lambda$ , even for electrospinning numbers  $\Gamma$  above the critical value  $\Gamma_c$ , by the universal relationship (10). Moreover, this approach reveals the universal relationship between the dimensionless relaxation time  $T$  and electrospinning number  $\Gamma$ , viz., Eq. (11). The introduced theory is surprisingly powerful not only for electrospinning from free liquid surfaces, viz., Fig. 4, but also for the capillary process, as is shown on Fig. 3. From the curves in Fig. 3, it is evident that as the radius of the capillary increases, deviation of the diameter  $2r$  from the wavelength  $\lambda$  increases. It is probably because of the fact that with the increment of capillary diameter interference of multidirectional waves (as degree of freedom increases) has more prominent effect. In cleft spinner since the waves are mostly unidirectional, such concept of superposition seems to be redundant.

The authors aimed at bringing about the simplest de-

scription of electrospinning from free liquid surfaces, based on the classic dispersion law. Remarkably, the dispersion law has been derived under the strongly simplified assumptions. Among them, the premise that “the amplitude  $a$  of the wave is *initially* negligibly small, as compared to its wavelength  $\lambda$ ,” is the most provoking one since electrospinning jets are, according to the hypothesis, created from crests of the exponentially growing wave. These apparently contradictory remarks may be apprehended in the context of fastest forming instability of the system’s self-organization. It may be considered that the temporal growth of the instability is too quick; hence, it keeps its characteristic wavelength even in its evolution stages that are far from conditions under which the instability is initiated. It is relevant to underline here that the analysis of the well-known Rayleigh instability of the spontaneous detachment of liquid films on cylindrical bodies into regular isolated droplets is based on a quite similar assumption.

Eventually, it is worth mentioning that the strong correlation between field strength and number density of jets unveils the scope of engineering spinner geometry and liquid properties for developing newer nanoscale fibrous materials and electrospinning technologies. This theory has a wider scope of development regarding thickness of the liquid layer from which electrospinning operates, introduction of viscosity and connected nonlinearities, and also interactions of waves on two-dimensional liquid surfaces.<sup>24</sup> It may appropriately be pointed out that even the present one-dimensional model of electrospinning is not entirely free from interference between two fastest forming waves. These waves may also have opposite directed motions just before the criticality is reached. Constructive wave interference that has been neglected in the work, intuitively leads to a decrease of critical voltages and, hence, it increases the local field strength values in the vicinity of interfered wave crests that may have bigger amplitude than the original ones.

## ACKNOWLEDGMENTS

We are thankful to The Ministry of Education of the Czech Republic (project No. CEP1-1M0554) for their support in the frame of The Research Centre for Advanced Conservation Technologies. The authors also thank the Czech company ELMARCO for additional financial support of their research. The authors feel obliged to the members of The

Department of Nonwovens, TUL, specifically, to F. Sanetrnik, for his invaluable assistance. It would also not be out place to express our gratitude to A. Linka and M. Tunak from The Department of Textile Materials, TUL, for their valued suggestions in analyzing the images obtained with movie camera in order to measure the average interjet gaps. We will fail in our duties if we do not acknowledge the contributions of J. Bhasin and A. Garg from IIT Delhi and K. Sachar from NIT Jalandhar in experimentation; and to L. Ocheretna of The Department of Textile Evaluation, TUL, for her drawing the graphics.

- <sup>1</sup>J. Lannutti, D. Reneker, T. Ma, D. Tomasko, and D. Farson, *Mater. Sci. Eng.*, **C 27**, 504 (2007).
- <sup>2</sup>M. Li, M. J. Mondrinos, M. R. Gandhi, F. K. Ko, A. S. Weiss, and P. I. Lelkes, *Biomaterials* **26**, 5999 (2005).
- <sup>3</sup>E. Kenawy, F. I. Abdel-Hay, M. H. El-Newehy, and G. E. Wnek, *Mater. Sci. Eng., A* **459**, 390 (2007).
- <sup>4</sup>J. Zeng, X. Xu, X. Chen, Q. Liang, X. Bian, L. Yang, and X. Jing, *J. Controlled Release* **92**, 227 (2003).
- <sup>5</sup>Z. Ma, M. Kotaki, and S. Ramakrishna, *J. Membr. Sci.* **265**, 115 (2005).
- <sup>6</sup>R. Gopal, S. Kaur, Z. Ma, C. Chan, S. Ramakrishna, and T. Matsuura, *J. Membr. Sci.* **281**, 581 (2006).
- <sup>7</sup>G. F. Taylor and M. D. Van Dyke, *Proc. R. Soc. London, Ser. A* **313**, 453 (1969).
- <sup>8</sup>J. Zeleny, *Phys. Rev.* **3**, 69 (1914).
- <sup>9</sup>P. K. Baumgarten, *J. Colloid Interface Sci.* **36**, 75 (1971).
- <sup>10</sup>O. Jirsak, F. Sanetrnik, D. Lukas, V. Kotek, L. Martinova, and J. Chaloupek, U.S. Patent No. WO2005024101 (17 March 2005).
- <sup>11</sup>A. L. Yarin and E. Zussman, *Polymer* **45**, 2977 (2004).
- <sup>12</sup>B. Alberts, D. Bray, A. Johnson, J. Lewis, M. Raff, K. Roberts, and P. Walter, *Essential Cell Biology* (Garland, New York, 1998).
- <sup>13</sup>A. Formhals, U.S. Patent No. 1,975,504 (14 January 1934).
- <sup>14</sup>S. A. Theron, A. L. Yarin, and E. Zussman, *Polymer* **46**, 2889 (2005).
- <sup>15</sup>O. Jirsak, K. Kalinova, and D. Stranska, *VDI-Ber.* **1940**, 41 (2006).
- <sup>16</sup>M. Stoneham, *Rep. Prog. Phys.* **70**, 1055 (2007).
- <sup>17</sup>L. D. Landau and E. M. Lifshitz, *Electrodynamics of Continuous Media*, 2nd ed. (Butterworth-Heinemann, Oxford, 1984).
- <sup>18</sup>L. D. Landau and E. M. Lifshitz, *Fluid Mechanics*, 2nd ed. (Butterworth-Heinemann, Oxford, 1987).
- <sup>19</sup>R. P. Feynman, *The Feynman Lectures on Physics* (Addison Wesley, Boston-San Francisco, 2005), Vol. 2.
- <sup>20</sup>A. W. Adamson and A. P. Gast, *Physical Chemistry of Surfaces* (Wiley, New York, 1997).
- <sup>21</sup>P. G. de Gennes, F. Wyart-Brochard, and D. Quere, *Capillarity and Wetting Phenomena; Drops, Bubbles, Pearls, Waves* (Springer-Verlag, New York, 2003).
- <sup>22</sup>S. L. Shenoy, W. D. Bates, H. L. Frisch, and G. E. Wnek, *Polymer* **46**, 3372 (2005).
- <sup>23</sup>S. Ramakrishna, K. Fujihara, W. Teo, T. Lim, and Z. Ma, *An Introduction to Electrospinning and Nanofibers* (World Scientific, Singapore, 2005).
- <sup>24</sup>A. L. Pregonzer and B. M. Marder, *J. Appl. Phys.* **60**, 3821 (1986).